The 14th International Topical Meeting on Nuclear Reactor Thermalhydraulics, NURETH-14
Toronto, Ontario, Canada, September 25-30, 2011

NURETH14-30

EXPERIMENTAL INVESTIGATION OF NUCLEATE BOILING ON HEATED SURFACES UNDER SUBCOOLED CONDITIONS

C. Schneider[1], R. Hampel[1], A. Traichel[2], A . Hurtado[3], S. Meissner[3], E. Koch[3],
[1] University of applied Sciences, Zittau/Görlitz, Saxony, Germany
[2] Nukem Technologies GmbH, Alzenau, Bavaria, Germany
[3]Technische Universität Dresden, Saxony, Germany

Abstract

In case of an accident at pressurized water reactors (PWR), critical boiling conditions can appear at the transition from bubble- to film boiling. During full power operation, heat transfer phenomena of sub cooled nucleate boiling occur on the surface of the fuel rods. To investigate the microscopic processes in nucleate boiling, a test facility with optical measuring methods was constructed. This allows analyzing the effects on a single bubble system at different parameters. For the generation of nucleate boiling, an optically transparent, electrically conductive coating was applied as a heating surface on a borosilicate substrate. The so-called ITO (Indium-Tin-Oxide) coating with a sheet resistance of 20 ohms enables an electrical heating at an optical transparent surface. These properties are prerequisites for the study of microscopic phenomena in the bubble formation with optical coherence tomography (OCT). OCT, generally used in medical diagnostics, is an imaging modality providing cross sectional and volumetric high resolution images. To make sure that the bubble formation takes place at a specific site, artificial nucleation sites in form of micro cavity will be inserted into the surface. Furthermore a small test facility was constructed to dedicate the wall temperature of a heated metal foil during subcooled boiling in non degassed water, which is the content of this paper.

Introduction

Nucleate boiling is an effective way to increase the heat flux from heated surfaces into the cooling liquid. Also the heat transfer occurs at small temperature differences and could be hold constant during variation of the heat flux [1, 2]. By increasing the heat flux, the bubble site density on the heated surface also increases until a maximum is reached, which is called critical heat flux (CHF). At this point, the vapor bubbles begin to combine to a closed film which covers the heating surface. The consequence is that the heat transfer decreases in cause of the isolating vapor film, which hinders the heated wall to be cooled by following fluid. In systems with impressed heat flux, like a nuclear reactor, the wall temperature rises rapidly by the transition from nucleate- to film boiling. This can lead to destruction of the fuel rods [5]. To minimize the risk of such accidents, conservative assumptions with large safety factors are currently used for the design of heat transfer in nuclear reactors. To predict the heat flux during pool boiling and flow boiling up to CHF, numerous correlation models have been developed by means of experimental investigations over the last few decades.
P.K. Jain [4] developed a method for the calculation of void fraction in forced convective subcooled boiling in heated annular channels. For this, he used the refrigerant R 113 as working

fluid. M. Gie Kang [6] investigated the effects of tube length on the nucleate pool boiling heat transfer coefficient. In experiments under atmospheric pressure he developed empirical correlations using various combinations of major parameters for application to advanced light water reactors. The results show that a shorter tube length is more efficient to increase heat transfer rate. G. A. Hughmark [7] correlated heat transfer coefficients for liquid inside tubes during forced-convection boiling or condensation in terms of the properties of pure components. T. Okawa [8] developed a new set of correlations for the film flow model to predict the critical heat flux in annular flow regimes accurately. To test the performance of his model, experimental data of critical heat flux in forced flow of water in vertical uniformly heated tubes were used.
All these correlations describe the global effects of heat transfer and mostly applicable for the boundary conditions they are investigated for. On the other hand, the errors between calculated and experimentally determined CHF accounts for up to 30 %.
To make a more exactly declaration of boiling heat transfer on heated surfaces, a consideration of the microscopic phenomena of single bubbles are required. To model the heat flux on a single bubble system, the so called wall boiling model is used. The mechanistic flow boiling model is based on local parameters (liquid velocity, temperature, turbulence intensity and void fraction) and is independent of the geometry of the heated channel. This model takes into account the processes that are encountered during the ebullition cycle in a simplified way and is divided into 3 partial heat fluxes (Fig. 1).

1. The convective heat flux $\dot{q}_F$, which occurs without evaporation.
2. the evaporation heat flux $\dot{q}_E$, which describes the heat and mass transport into the growing bubble, and
3. the quenching heat flux $\dot{q}_Q$, which describes the cooling of the heated surface in cause of the bubble detachment and flow of relatively cool liquid to the nucleation site [9].

Physical processes, which take place in the microstructure of a growing vapor bubble, are not totally understood and still plagued with large uncertainties. Different and often contradictory hypotheses have been proposed to describe the nature of surface heat transfer during the bubble formation and departure process. The necessary experimental tools to test the basic assumptions are not available in a sufficient spectrum [10]. To develop so called CFD wall boiling models to describe the phenomena between heated surface, liquid and growing bubble a basis of experimental data will be needed. Simultaneous visualization and measurement of the surface

$$\dot{q}_W = \dot{q}_F + \dot{q}_E + \dot{q}_Q$$

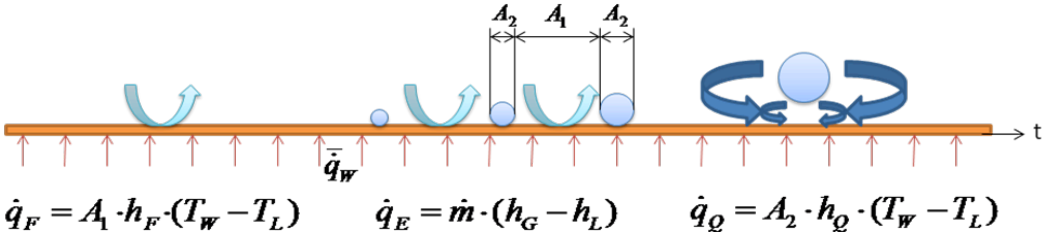

Figure 0 Concept of wall boiling model, the wall heat flux $\dot{q}_W$ consists of the convective heat flux $\dot{q}_F$, the evaporation heat flux $\dot{q}_E$ and the quenching heat flux $\dot{q}_Q$

temperature are required to demonstrate the coherence between bubble behavior with global and local heat fluxes. The measured parameters should include, among others, the wall temperature on micro- and macro- scale, the ebullition cycle with quantifying parameters like waiting time, bubble growing time, sliding time and bubble diameter history [9].
This experimental analyzing is focused on subcooled nucleate boiling in water under atmospheric pressure. To quantify the wall temperature and the distribution of the different heat fluxes during the ebullition cycle, infrared thermography is used.

1. Experimental Setups

For the evaluation and development of the measurement techniques and investigation of nucleate boiling, different test facilities are constructed. The first pretests are necessary to investigate the applicability of the temperature measurement on thin heated surfaces and the bubble detection with Infrared Thermography (IR). This information is used to develop a first evaluation algorithm to quantify the spatial heat fluxes. This facility was also used for the investigation of different artificial nucleation sites on optical transparent, electrically heated surfaces.

1.1 Nucleate boiling under forced convection

For investigating nucleate boiling under forced convection, a test facility was constructed for the measurement with video imaging, OCT and IR. The working fluid is distilled water under atmospheric pressure. This test facility consists of the components shown in Fig. 2. A special pump a) with a NPSH value below 0.5 m at a maximum flow rate of 6 m^3/h is used to transport the water in a circuit. The low NPSH is necessary to realize a possible high input temperature without danger of cavitation at the entrance of the pump. In the following preheating b), with a maximum power of 10 kW, the water is heated up to reach entrance temperature near saturation conditions. The test section c) consists of a rectangular flow channel with optical access in four directions. With dimensions of 28 x 28 mm and a length of 350 mm, a maximum flow velocity of approximately 2 m/s can be realized, which is captured with a paddlewheel flow meter d). Three sites of the channel are made of borosilicate glass to get optical access to the heating surface, which is implemented in the back panel. The back panel contains a borosilicate substrate window with an electrical conductive and optically transparent coating. The Indium Tin Oxide (ITO)-layer has a surface resistance of 20 Ohm and provides a transmission until above 1400 nm.

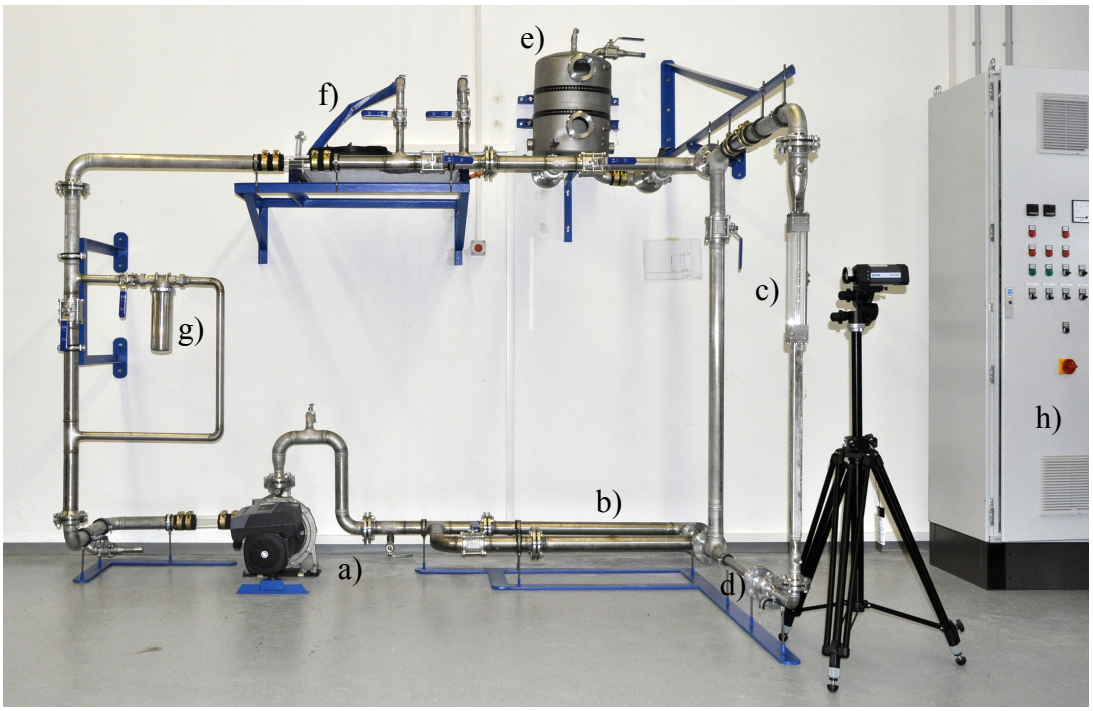

Figure 2 Test facility for investigation of nucleate flow boiling; a) pump, b) preheater, c) test section; d) flow meter, e) degasser, f) cooler, g) filter, h) control box

To generate single bubbles on a defined site an artificial nucleation site will be inducted into the surface. For acquisition of nucleate boiling conditions on different heated surfaces the back panel can be changed for the adoption of alternative geometries. One of the most important components of the test facility is the thermal degasser d) with two heat elements, each with a power of 2.5 kW. Before starting the experiment, the water should be degassed from inert gases by boiling over a time of approximately 2 h [12]. After that, the water will be injected into the facility. It will be degassed continuously during the experiments by distributing a part mass flux through the degasser. The cooler is necessary for the back cooling of the water on a sufficient subcooling to avoid cavitation in the pump. A filter ensures the removal of particles that can act as nucleation sites and distort the measurement results.

1.2 Pretest 1

The simple pretest facility consists of a rectangular water pool with three glass walls and one wall of thermal stable polymer (Fig. 3). In this wall are inserted two holes with a diameter of 10 mm. These holes are masked by an aluminum foil with 10 µm and a copper foil with 35 µm thickness. The foils are connected to an AC power supply with a maximum of 9 V and 250 A, so they are heated electrically by their inherent resistance. The pool is filled with water whereat the foils are caulked against water outlet. The backsides of the foils are coated with a matt black paint to ensure a defined emission of 96 % for the IR measurement. The very thin foils afford that the measured temperature distribution on the backside of the foils shows only small variations from the temperature signal at the front side where the evaporation takes place [11]. In this pretest no artificial nucleation site is inserted, so random nucleation sites are detected, measured, and investigated. For the measurement of the wall temperature, an IR camera with a

spectral range of 7.5 – 14 µm is used to measure the heating wall temperature and detect growing bubbles in shape of cooled spots. The IR camera is connected by Ethernet to the PC that captures the IR images as a matrix of specific spectral radiance. With the provided software, the temperature is calculated in dependence of emissivity, distance and reflected temperature of the object, temperature and relative humidity of atmosphere and temperature and transmission of the external optics. The camera is equipped with a macroscopic objective which provides a spatial resolution of approximately 75 µm/pixel. With a pixel resolution of 320 x 240 the field of view amounts to 24 x 18 mm. The temporal resolution of the camera can be increased up to 60 Hz. To eliminate noise, a special filter from the digital image processing is used, which is described in the 3th paragraph.

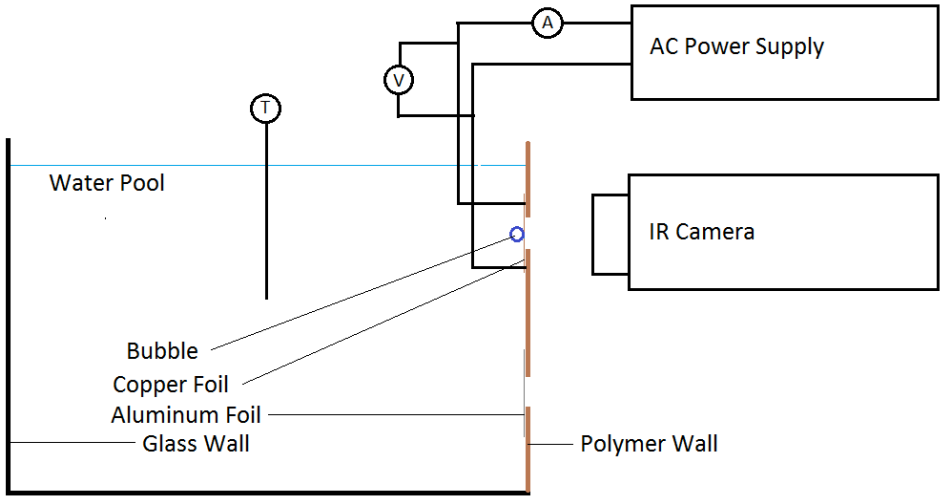

Figure 3 Pretest facility for determination of wall temperature

2. Analysis of wall temperatures

2.1 Slow growing bubble

In the first experiment, the temperature of a heated aluminum foil is measured during a very slow growing bubble. The IR pictures are taken with a frame rate of 30 Hz whereat the subcooling amounts 46 K and the foil is heated with 70 W at 50 A. The calculated electrical heat flux density on this surface equates approximately to 4.6 W/cm². As shown in Fig. 4 the growing of the bubble begins on a stochastic nucleation site. The very slow growing can be considered as quasi-stationary. So the gas film of the bubble isolates the heated surface to be cooled by the fluid at this location. This can be seen on the IR-picture as a spot of higher temperature. The surface temperature around the bubble is some 89 °C, this shows that the fluid temperature on the heated wall is already in a subcooled condition. So the rising bubble has mainly to consist of inert gases which are dissolved in the water. The growth of the bubble takes place over a period of about 100 s. The temperature in the area of the bubble rises depending on their size, because the thickness of the isolating layer increases. Furthermore, the bubble slides slowly above during the rising whereat a new bubble begins to grow on the primary nucleation site of the first. The

subsequent sudden detachment of the newly formed bubble causes a strong local cooling by the replenished flow of subcooled liquid. This fast local cooling causes the so-called quenching heat flux. As shown in Fig. 5, the cooling during the first time step of detachment amounts to a difference of maximum 7 K in 34 ms. In the next time steps, the lift of the small bubble causes entrainment of the big bubble, which detaches subsequent. In this way, the heated surface is cooled in a bigger area because of the enhanced convection during the lift of the big bubble. After this detachment, the surface heats up again and the next bubble is growing on the nucleation site.

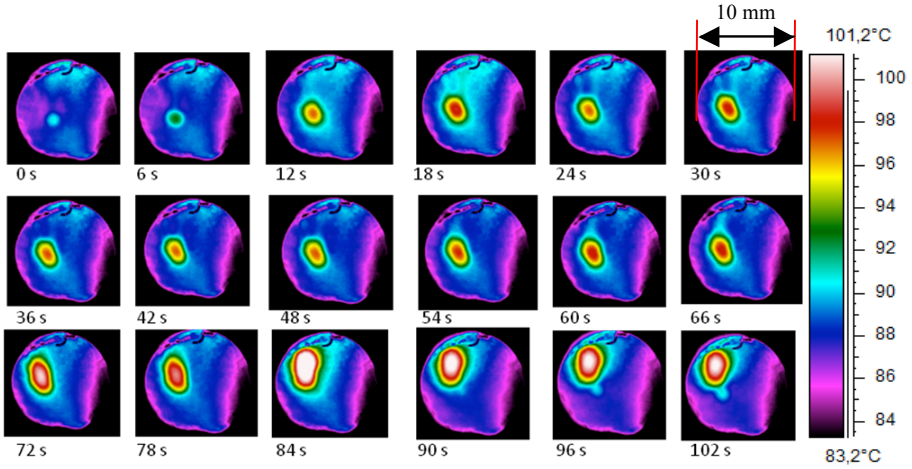

Figure 4 Slow bubble growing, q_{el}=4.6 W/cm²

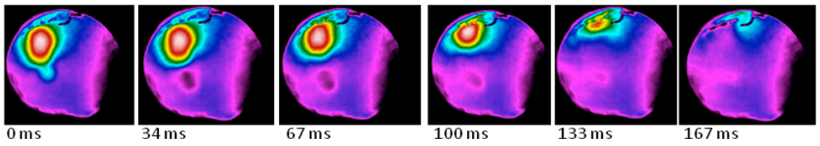

Figure 5 Detachment of the second bubble and entrainment of the first

2.2 Fast growing bubble

The rising of the heat flux causes the increasing of nucleation site density and detachment frequency as well as the detachment diameter decreases. This causes a locally and temporally smoother distribution of the temperature changes due to bubble growing and detachment. The result is a lower local influence of the surface temperature which makes the detecting of a single bubble much more difficult. So the influence of the noise rises up and the surface temperature becomes more homogeneous during nucleate boiling.

During the measurement, one bigger bubble could be detected to investigate the changes of the local surface temperature on the copper foil. In this experiment, the foil is heated with 190 W and a current of 200 A. In Fig. 6, the local change of the surface temperature during a fast bubble growing and detachment is shown. The calculated electrical heat flux density on this surface equates approximately to 11.65 W/cm². Compared with slow growing the temperature difference during the bubble cycle is much smaller. It only amounts to 3.25 K, what depends on the smaller detachment diameter and higher frequency. Also the bubble detachment could not be divided from the evaporation process, so the cooling of the surface is seen as the complete cycle. With a

frame rate of 60 Hz it is still difficult to locate local temperature changes caused by individual bubbles. The average surface temperature amounts to 114 °C. As the saturation temperature at atmospheric pressure is 100 °C, the wall superheat amounts to 14 K.

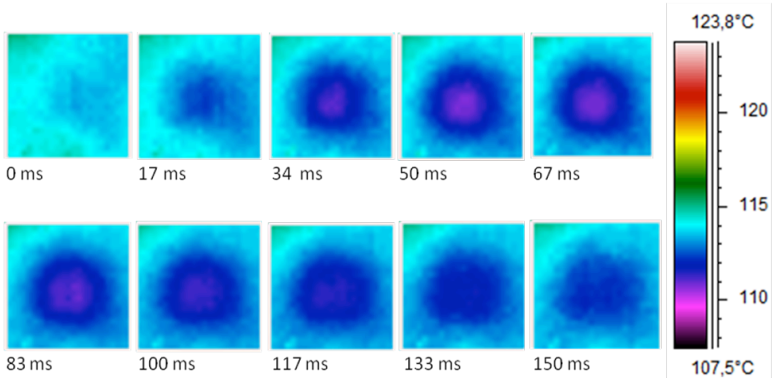

Figure 6 Wall temperature distribution under fast bubble growing and detachment, q_{el}=11.65W/cm²

3. Calculation of surface heat flux

For the determination of the increased local heat flux as cause of bubble growth and detachment, the energy balance is solved for each volume element of the foil. An analog application concerning nucleate boiling on thin heating foils is used in [1, 2]. These elements are rendered by the pixel size of the IR picture and the thickness of the foil. So the considered volume elements have scale dimensions in the x and y axes of 75 x 75 µm and a height which corresponds to the film thickness of 15 µm for aluminum and 35 µm for copper. While the backside is considered as adiabatic, in the x- and y-direction additional heat fluxes have to be assumed due to heat conduction to the adjacent elements. A constant heat flux q_{el} is given by the converted electric power. The storage of thermal energy by heating or the short-term provision of high heat fluxes through cooling of the volume element is to be regarded as an essential mechanism in nucleate boiling. A general balance according to the first law of thermodynamics, including the Fourier's heat conduction equation, is Eq. (1).
The temperature T is considered to be constant within the volume element. The result is the wanted unknown value of local heat flux $\dot{q}_B$, which is transferred from the heating wall to the boiling liquid. For the actual case, the heat storage is determined by comparing the temperatures between two moments, where k is the time step in Eq. (2). The time step between two pictures $\Delta\tau$ results from the frame rate of the IR camera Eq. (3). By multiplying with the film thickness δ_{HF}, a heat flux $\dot{q}_{sp}$ can be presented in this way, which only results of cooling and heating of the foil. If the considered volume element is on a different temperature level than its adjacent elements, a heat flux $\dot{q}_{leit}$ will appear due to the high thermal conductivity to balance the temperature gradient. For the double derivative in x-direction, the approximation Eq. (4) is adopted. The calculation of the heat flux in y direction occurs analog.

$$\underbrace{\delta_{HF}\rho c\frac{\partial T}{\partial \tau}}_{\dot{q}_{sp}} = \underbrace{\lambda\delta_{HF}\left(\frac{\partial^2 T}{\partial x^2}+\frac{\partial^2 T}{\partial y^2}\right)}_{-\dot{q}_{leit}} + \dot{q}_{el} - \dot{q}_B \qquad (1)$$

$$\frac{\partial T}{\partial \tau} = \frac{T_{k+1} - T_k}{\Delta \tau} \tag{2}$$

$$\Delta \tau = \tau_{k+1} - \tau_k = \frac{1}{f_{cam}} \tag{3}$$

$$\frac{\partial^2 T}{\partial x^2} \approx \frac{T_{i+1} - 2T_i + T_{i-1}}{(\Delta x)^2} \tag{4}$$

3.1 Detachment of slow growing bubble

During the detachment of the slow growing bubble at low heat flux (Fig. 5), the quenching by cooling is calculated for each time step. In Fig. 7 it is shown that the local cooling of the surface at the moment of the small bubble detachment causes an additional heat flux of up to 0.6 W/cm², based on the time step of 34 ms. Because of the subsequent detachment of the large bubble, it can be seen that the levels of the local heat flux distribution expand to a wider range. Furthermore, the additional heat flux increases up to 1.2 W/cm² after 167 ms. This shows the increased heat transfer which is caused by secondary vortices due to the detaching and rising bubble [14]. As described in chapter 2.1, the growing bubble has to consist of dissolved inert gases that are visible on the highest temperature of the heated wall, which is still below the boiling temperature of water. Because of the very slow growing bubble, which can be considered in steady state, it could be adopted that the additional heat flux only depends on the quenching caused by bubble detachment. So these methods enable to investigate the local quenching heat flux without the additional influence of evaporation.

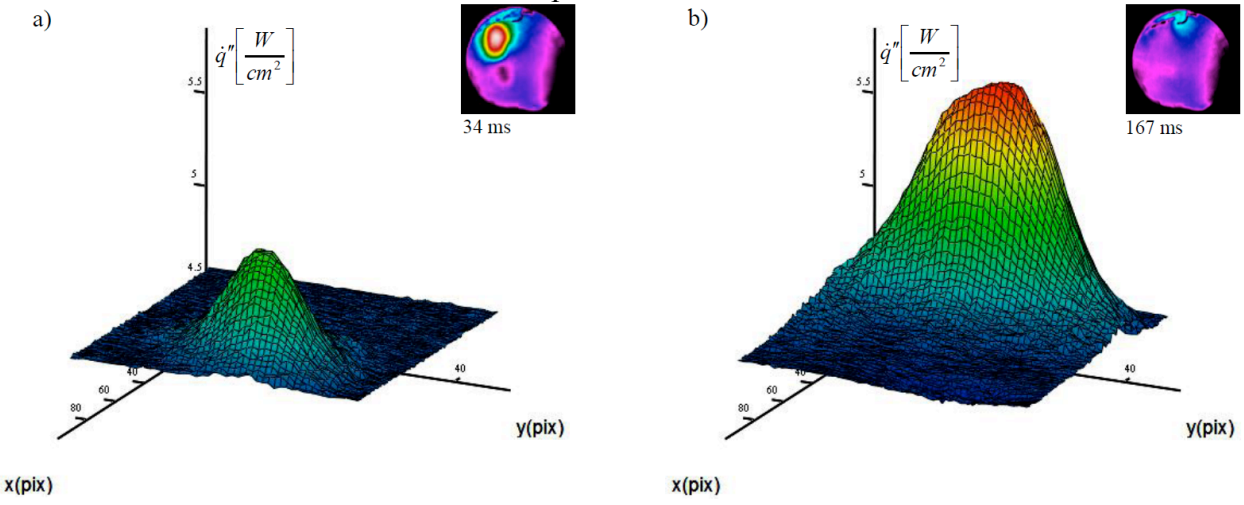

Figure 7 Additional heat flux during a) detachment of the small- and b) entrainment of the big bubble

3.2 Ebullition cycle of fast growing bubble

For the calculation of the total heat flux during the ebullition cycle of a fast growing and detaching bubble, a small area is picked out for the investigation. The different heat fluxes as cause of constant electrical heating, storage heat flux as cause of local, temporal cooling of the foil and conductive heat flux resulting from the temperature gradients on the surface are calculated.

The local cooling of the surface causes a local heat flux from the storage of the copper foil (Fig. 8) which is calculated with Eq. (1). As seen, the maximum heat flux of storage in the foil is lower than the heat flux during the bubble detachment of the small, slow growing bubble (Fig. 7) and amounts to 0.49 W/cm². This shows that the lower heat flux of storage depends on the smaller detachment diameter and higher frequency. Nevertheless, due to the higher frequency the waiting time for a new bubble is much shorter. So in a specific time more evaporation cycles take place which increases the global heat flux. In this way a higher total heat flux is transferred from the foil to the liquid.

The conductive heat flux because of the temperature gradients between each foil element is shown in Fig. 9. In this diagram it can be seen that the heat flux has a very uneven distribution. This property is related to the signal noise of the temperature detection by the IR camera. To smooth this noise filtering of the values is necessary. In this case, a so-called Gauss-filter from the digital image processing was used. After filtering, the heat flux with different filters such as average- and median-filter, the Gaussian-filter enabled the best smoothing with minimum deviation. For the filter method, a 5 x 5 filter operator has been used, see Eq. (5). Due to the filtering operation Eq. (7), each value of the image matrix will be recalculated by including the surrounding values and allocation of appropriate weights. In this case, N is the sum of the filter coefficients Eq. (6), where L and K are the dimensions of this filter operator. B is the respective target point where x and y describe the image coordinate whereat u is the row index and v the column index of the filter operator [15,16]. The result of the filter operation is shown in Fig. 10. This operation causes a much smother heat flux distribution with an enhanced flux in the bubble center. The average deviation of the temperatures by smoothing amounts 0.075 K, the maximum error amounts 0.759 K. So the relative average deviation amounts 1.5 % in comparison to a local cooling by 5 K. It can be seen that the conductive heat flux with a maximum value of 46.2 W/cm² is much bigger than the storage heat flux.

$$h = \begin{pmatrix} 1 & 4 & 6 & 4 & 1 \\ 4 & 16 & 24 & 16 & 4 \\ 6 & 24 & 36 & 24 & 6 \\ 4 & 16 & 24 & 16 & 4 \\ 1 & 4 & 6 & 4 & 1 \end{pmatrix} \tag{5}$$

$$N = \sum_{u=0}^{L-1} \sum_{v=0}^{K-1} h_{u,v} \tag{6}$$

$$g(x,y) = \frac{1}{N} \sum_{u=0}^{L-1} \sum_{v=0}^{K-1} \left(B_{x-l+u,\, y-k+v} \cdot h_{u,v} \right) \tag{7}$$

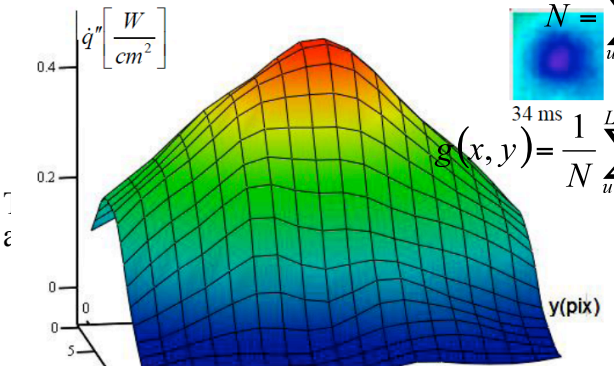

Figure 8 Additional storage heat flux in foil

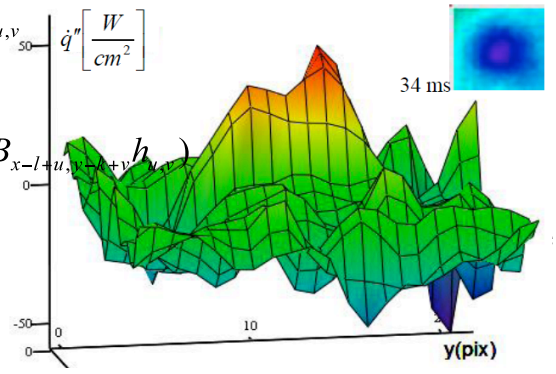

Figure 9 Unsmoothed conductive heat flux

ebullition cycle is composed of electrical, storage and conductive heat flux. Fig. 11 shows the local distribution of the total heat flux in the foil. It can be seen, that the main influence because of bubble formation results from the temperature gradients in the surface of the heated foil.

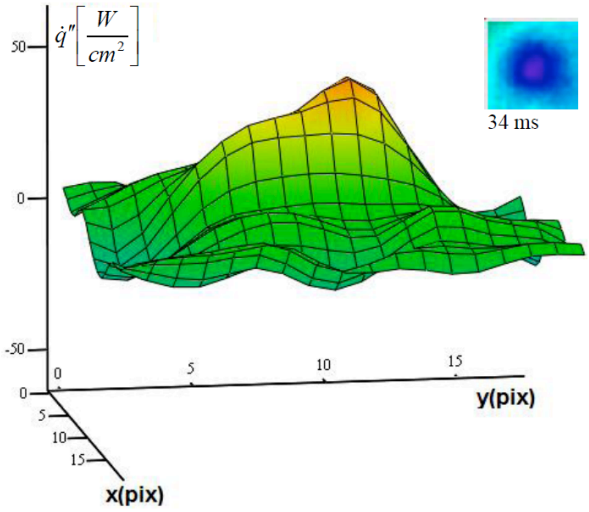

Figure 10 Smoothed conductive heat flux in foil

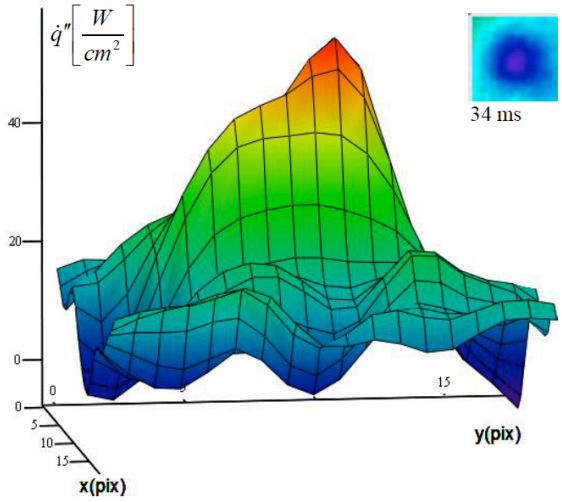

Figure 11 Total Local heat flux distribution

4. Conclusion and outlook

In these work, methods for the investigation of parameters for the modeling of wall boiling processes were presented. With the acquisition of local changes of the wall temperature by infrared measurement during bubble growing and detachment, heat fluxes are calculated. The individual heat fluxes resulting from the storage and conductive heat flux in the foil are calculated during evaporation and detachment of fast growing bubbles as well as only quenching heat flux in cause of very slow growing and fast detaching bubbles. These bubbles are generated of dissolved inert gases without evaporation of water so that the evaporation heat flux can be neglected. The uneven calculated heat flux distribution because of signal noise could be smoothed with the Gaussian- filter of digital image processing with mean error of 1,5%.
The next steps of this project are the synchronous imaging of the bubble formation with IR- and CMOS-camera to quantify the local heat fluxes more exactly. By measuring the bubble frequency and the detachment diameter with a CMOS- camera, the heat flux, which is transported into the bubble during evaporation, can be calculated. With the measurement of the local and global wall temperature distribution the heat fluxes from the heated wall during different boiling conditions can be quantified. Together with the convective heat flux on the surface the quenching heat flux can be calculated for the further development of the wall boiling models in CFD. This needs results from lack of detailed experiments with flow boiling, which would focus on the ebullition cycle [9].

Acknowledgement

This work is supported by the German Federal Ministry of Education and Research (BMBF) within the joint project “fundamental research Energy 2020+” under project number “02NUK010C” and “02NUK010I”

5. References

[1] E. Wagner, 2008, Hochauflösende Messungen beim Blasensieden von Reinstoffen und binären Gemischen, Dissertation, Fachbereich Maschinenbau, Technische Universität Darmstadt

[2] I. Golobic, et al., 2007, Experimental determination of transient wall temperature distributions close to growing vapor bubbles, Heat Mass Transfer (2009) Vol. 45, pp. 857-866

[3] W. Qu, et al., 2003, Measurement of critical heat flux in two-phase micro channel heat sink, Heat Mass Transfer (2004) Vol. 47, pp. 2045-2059

[4] P.K. Jain, 1980, A study of forced convective subcooled boiling in heated annular channels, Nuclear Engineering and Design (1980) Vol. 60, pp. 401-411

[5] D. Schroeder-Richter, et al., Analytic calculation of DNB-superheating by a postulated thermo-mechanical effect of nucleate boiling, Multiphase Flow (1994) Vol. 20, No. 6, pp. 1143-1167

[6] M. Gie Kang, 1997, Experimental investigation of tube length effect on nucleate pool boiling heat transfer, Ann. Nucl. Energy (1998) Vol. 25, No. 4-5, pp. 295-304

[7] G. A. Hughmark, 1984, Heat transfer with phase changes in vertical upward, horizontal, and vertical downward tube flow, Ind. Eng. Chem. Fundam. 1982, Vol. 21, pp. 339-343

[8] T. Okawa, et al., 2003, Prediction of critical heat flux in annular flow using a film flow model, Nuclear Science and Technology, 2003, Vol. 40, No. 6, pp. 388-396

[9] H. Anglart, 2007, FZD Fellowship: Topics of Work

[10] S. Maghaddam, et al., 2008, Physical mechanism of heat transfer during single bubble nucleate boiling of FC-72 under saturation conditions –I. Experimental investigation, Heat and Mass Transfer, 2009, Vol. 52, pp. 1284-1294

[11] C. Sodtke, et al., High resolution measurement of wall temperature distribution underneath a single vapour bubble under low gravity conditions, Heat and Mass Transfer, 2006, Vol. 49, pp. 1100 -1106

[12] R. Maurus, 2003, Bestimmung des Blasenverhaltens beim unterkühlten Sieden mit der digitalen Bildfolgeanalyse, Dissertation, Lehrstuhl für Thermodynamik, Technische Universität München

[13] K. Fuechsel, 2009, Optical Properties of ITO Thin Films Produced by Plasma Ion-Assisted Evaporation and Pulsed DC Sputtering, Fraunhofer-Institute for Applied Optics and Precision Engineering IOF, Jena, Germany

[14] K. Stephan, 1988, Wärmeübergang beim Kondensieren und beim Sieden, Springer

[15] B. Neumann, 2005, Bildverarbeitung für Einsteiger, Springer

[16] C. Demant, et al., 1998, Industrielle Bildverarbeitung, Springer

SPONSORED BY THE
Federal Ministry of Education and Research